Sliding over a Phase Transition

A. Benassi,[1,2] A. Vanossi,[2,1] G. E. Santoro,[2,3,1] and E. Tosatti[2,3,1]

[1]*CNR-IOM Democritos National Simulation Center, Via Bonomea 265, I-34136 Trieste, Italy*
[2]*International School for Advanced Studies (SISSA), Via Bonomea 265, I-34136 Trieste, Italy*
[3]*International Centre for Theoretical Physics (ICTP), P.O. Box 586, I-34014 Trieste, Italy*

(Received 27 April 2011; published 22 June 2011)

The effects of a displacive structural phase transition on sliding friction are in principle accessible to nanoscale tools such as atomic force microscopy, yet they are still surprisingly unexplored. We present model simulations demonstrating and clarifying the mechanism and potential impact of these effects. A structural order parameter inside the material will yield a contribution to stick-slip friction that is nonmonotonic as temperature crosses the phase transition, peaking at the critical T_c where critical fluctuations are strongest, and the sliding-induced order-parameter local flips from one value to another more numerous. Accordingly, the friction below T_c is larger when the order-parameter orientation is such that flips are more effectively triggered by the slider. The observability of these effects and their use for friction control are discussed, for future application to sliding on the surface of and ferro- or antiferrodistortive materials.

DOI: 10.1103/PhysRevLett.106.256102 PACS numbers: 68.35.Af, 07.79.Sp, 62.20.Qp, 63.70.+h

Understanding and controlling nanoscale friction are among the top priorities in nanoscience and technology, where moving elements are increasingly important. Unearthing mechanisms capable of altering dry friction, to be employed in addition to traditional means such as lubrication, tuning of load, temperature, and speed [1], is of great interest in physics and for potential applications. The idea is to replace a ''dead'' substrate, with a purely passive role, with a ''live'' material hosting a phase transition. Early surface science work provided an indirect hunch, in the form of a predicted drop of the 2D diffusion coefficient D for a Brownian adsorbate particle, caused by an underlying surface phase transition [2–4]. In that case, Einstein's relation $D\eta = k_B T$ implies the prediction of a peak in the particle's viscous friction η at the surface critical temperature T_c^{surf}. Although this linear response is not realistically relevant to dry friction, dominated by nonlinear stick slip [1], that example is nonetheless suggestive of a frictional anomaly near a substrate phase transition. Experimentally, a spectacular anomaly is the critical frictional drop reported at the superconducting-normal transition of a metal substrate [5,6].

In some ferroelectrics such as TGS (triglycine sulfate) [7] and to a lesser extent $BaTiO_3$ [8], atomic force microscopy (AFM) topography and friction have shown contrast between surface domains. These systems are pestered with structural and electrostatic complications which one may wish to avoid at this first, more fundamental level. At that level, the basic questions are (i) what is the frictional coupling mechanism between tip motion and a substrate structural phase transition, (ii) what is the distinguishing element of the phase-transition related frictional contribution relative to the background friction, and (iii) could one achieve friction control through external fields that influence the substrate order parameter?

In order to explore these questions theoretically ahead of future experiments, we resort to a model study. Specifically, we carry out molecular dynamics (MD) classical simulations for the stick-slip dry friction of an idealized pointlike AFM tip over a two-dimensional (2D) model crystal substrate whose bulk undergoes a weak, continuous structural phase transition. Our chosen model will be one of a general ''displacive'' type, a category in principle describing popular systems such as some ferroelectrics [9,10].

Figure 1 sketches our model system, a 2D close-packed atomic lattice (the substrate) of classical particles (the atoms), and a point slider (the tip) pulled over the substrate edge (the surface) through a spring (the cantilever), as in a classic Tomlinson model [1]. The substrate atoms (of mass m) are held together at an average distance a by an interatomic pair potential U_{ij}, locally similar to a Lennard Jones (LJ) potential, $U_{ij} = -U + \alpha(|\mathbf{r}_i - \mathbf{r}_j| - a)^2 + \beta(|\mathbf{r}_i - \mathbf{r}_j| - a)^4$, an approximation which avoids complications including thermal expansion. Parameters α and β are obtained by fitting a LJ potential of depth U and radius a (U, a and the mass m, define our set of ''natural'' units). In an interval $[-0.1, 0.1]$ centered on the minimum at a, the fit yields $\alpha = 28.32U/a^2$ and $\beta = 784.35U/a^4$. In addition to the interatomic interaction U_{ij}, each atom is subject to a six-valley on-site potential U_i with the same symmetry as the lattice (see inset in Fig. 1) chosen such as to favor a small uniform distortion of all sites towards one of six equivalent valleys $\lambda = 1, \ldots, 6$ $U_i = U_M - \frac{2(U_M - U_m)}{a_0^2}(3\frac{x_i}{u_i} - 4\frac{x_i^3}{u_i^3})u_i^2 + \frac{U_M - U_m}{a_0^4}u_i^4$. Here $u_i^2 = x_i^2 + z_i^2$ is the displacement magnitude of the ith atom from the site center, a_0 is the distance between the minima and the center, and U_M and U_m are the height and the depth of maximum and minima ($U_M = 0.1U$, $U_m = -0.1U$, and $a_0 = 0.05a$). At low temperature $T \ll |U_M - U_m|$, the

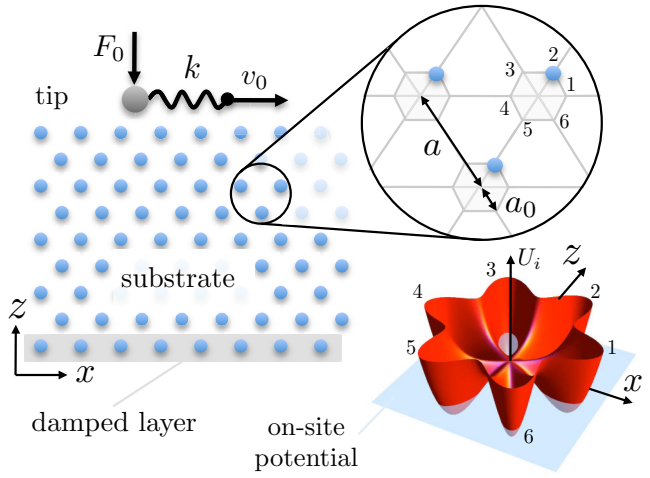

FIG. 1 (color online). Sketch of the 2D model system, the zoom shows the on-site potential symmetries, with the hexagon vertices representing its six valleys, displayed below.

ideal 2D lattice is characterized by the displacive vector order parameter $\boldsymbol{\delta}(T) = \langle \mathbf{u} \rangle = \langle \mathbf{r} - \mathbf{r}_0 \rangle$, measuring the average distortion $\mathbf{u}$ of atoms from the central triangular lattice positions $\mathbf{r}_0$. At $T = 0$, the substrate minimal energy state is at $|\boldsymbol{\delta}(0)| = a_0$, with all the atoms in the same valley λ, and $a_0/a \ll 1$. MD simulations of this model are carried out using 2D rectangular cells of large but finite thickness $L_z = N_z a\sqrt{3}/2$ along z and length $L_x = N_x a$ (typically $N_x = 40$, $N_z = 40$), first in thermal equilibrium, with bulklike periodic boundary conditions (PBC) applied along both x and z; then out of equilibrium, with PBC along x alone, the tip sliding taking place on one of two edges, in frictional simulations. We stress here our intent to mimic qualitatively the behavior of a real 3D system with a continuous phase transition, with the order parameter coupled to the slider's motion [11]. Models similar to the present one are successfully employed in the description of the displacive structural phase transitions of many systems, notably the very well known ferroelectric and distortive ones in the perovskites [9]. In bulk simulations which we carry out first (details in supplemental material [13]) the substrate equilibrium structural transition is identified by the vanishing (near $k_B T_c = 0.075U$) of the order parameter $\boldsymbol{\delta}(T)$, the peak of susceptibility components $\chi_{\alpha\beta} = -(\langle u_\alpha u_\beta \rangle - \langle u_\alpha \rangle \langle u_\beta \rangle)/K_B T$ and, slightly shifted due to finite size effects, the specific heat peak $C_V = (\langle E^2 \rangle - \langle E \rangle^2)/(K_B T^2 N_x N_z)$, where E is the internal energy. Below T_c, symmetry between the six valleys is broken and one of the six prevails. Just above T_c, symmetry is thermally restored and the distortion of each site, though instantaneously still present, is randomly distributed between all six valleys. Near T_c the system develops long correlations comparable with the simulation cell size, and its dynamics becomes correspondingly slow, as expected at a second order phase transition. In subsequent frictional simulations, the PBC along z are removed generating two free surfaces. The point "tip" of mass $M = 500$ m and coordinate $(X(t), Z(t))$, interacting with the substrate atoms via a LJ potential of depth $V \sim 0.6U$, is dragged over one surface at constant velocity $v_0 = 5 \times 10^{-3}\sqrt{U/m}$ through a spring of constant $k = 5U/a^2$, representing the cantilever lateral stiffness. A load force F_0 (typically of order 1 in units of U/a) is applied along z to press the tip onto the substrate. The overall equations of motion $m\ddot{X} = -\frac{dU_{\mathrm{LJ}}}{dX} - k(X(t) - v_0 t)$ and $m\ddot{Z} = -\frac{dU_{\mathrm{LJ}}}{dZ} - F_0$ are integrated with a velocity-Verlet algorithm with a time step $\Delta t = 5 \times 10^{-3}\sqrt{ma^2/U}$. The frictional Joule heat is removed by a standard Langevin thermostat endowed with an optimized viscous term $-m\gamma\dot{\mathbf{r}}$ and a corresponding random noise, both attached to the slab bottom layer only [14]. Simulation times are long enough for meaningful averages (no less than 50 stick-slip events required), but short enough to avert undesired order-parameter destruction due either to small size, or to the nucleation of defects heralding the onset of a Berezinskii-Kosterlitz-Thouless (BKT) state. The spring elongation $F_x(t) = -k(X(t) - v_0 t)$ measures the instantaneous friction force. Parameters of each frictional simulation are thus (a) the temperature T, (b) the overall substrate order-parameter valley $\lambda = 1, \ldots, 6$ for $T < T_c$, (c) the load F_0, (d) the average tip sliding speed v_0, and (e) the tip effective parameters such as mass M and stiffness k. Among these parameters, velocity is the least critical since stick slip is known to yield a nearly speed independent friction coefficient [15]. To cut computational costs, we generally adopt a rather large speed ($v_0 = 0.005\sqrt{U/m}$)—except when good quality stick-slip details are needed, requiring slower motion. Two tip mass values, $M = 500$ m (results shown here) or 5 m (supplemental material [13]), amounting to a factor 10 in cantilever frequency $\sqrt{k/M}$ again gave rather similar results. The dependence of friction upon the other parameters will be described next.

Primarily, we examine the lateral spring force $F_x(t)$, exhibiting for low speed a classic monoatomic stick-slip behavior (supplemental material [13]), close to that observed in realistic AFM nanofriction [15,16]. Its time average measures the dynamic friction and the corresponding friction coefficient $\mu \equiv \langle F_x(t) \rangle / F_0$. The overall behavior obtained for friction coefficient versus temperature, order-parameter valley, and load is presented in Fig. 2. First, the phase-transition-induced, temperature nonmonotonic stick-slip friction is confirmed, prominent here over the (temperature-monotonic) background friction. The friction coefficient broadly peaks in the neighborhood of the substrate phase transition, where friction rises substantially higher than at low temperature, to descend again at higher temperatures beyond T_c. Second, there is a clear dependence of friction upon the order-parameter valley in the substrate. That dependence, well visible for light loads at $T < T_c$, grows further with load (see upper and lower panels in Fig. 2). At large load and low temperature, the friction coefficient differs between valleys $\lambda = 1$ (or 4),

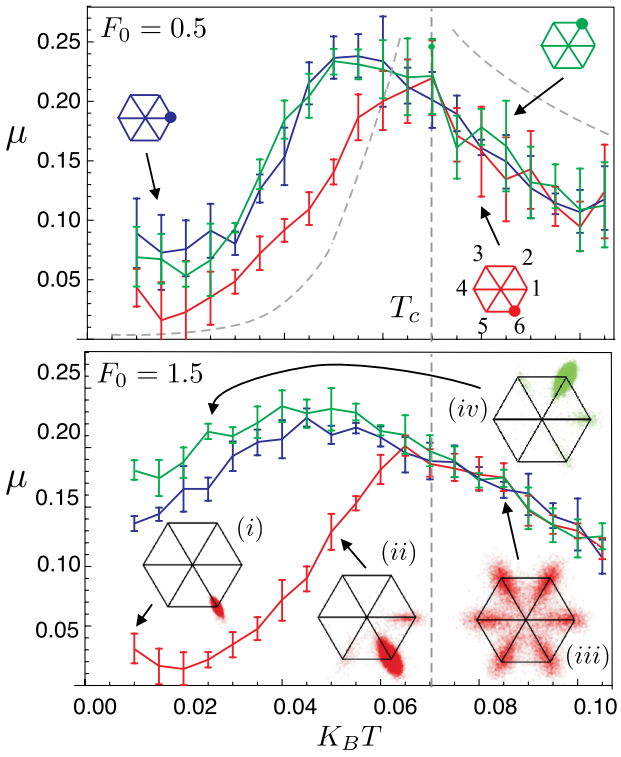

FIG. 2 (color online). Friction coefficient $\mu = \langle F_x \rangle / F_0$ versus temperature for different substrate order-parameter directions λ (correspondence as in upper panel). Hexagon occupancies in the lower panel illustrate the probability of the substrate "target atom" to be found in the six valleys of the on-site potential after ten stick-slip events. Upper and lower panels refer to two distinct load values. Dashed curve: bulk order-parameter static susceptibility $\frac{\chi_{zz}(\omega=0)}{a_0^2}$.

2 (or 3), and $\lambda = 6$ (or 5) by almost an order of magnitude. We stress that the friction nonmonotonicity versus T is here of a totally different nature from that recently demonstrated for multiple stick-slip regimes of motion [17], or for multicontact sliders [18].

So far we have discussed the simulation results. Is there a linear response theory that may explain them? Strictly speaking the answer is negative, because stick slip is a violent, nonlinear, nonuniform perturbation. In spite of that, it is instructive to compare the friction simulation data with a different kind of linear response theory. If the slider's speed, jerky because of stick slip, could be crudely replaced with a large uniform speed, itself unperturbed by the frictional processes, then a standard "golden rule" linear response could be invoked, predicting an average dissipated power $\langle P \rangle \propto \sum_{\mathbf{k}} \omega_{\mathbf{k}} |V_{\mathbf{k}}|^2 \chi''(\mathbf{k}, \omega_{\mathbf{k}})$, where $V_{\mathbf{k}}$ is the coefficient of the Fourier expansion of the slider-substrate potential, $\omega_k = \mathbf{k} \cdot \mathbf{v}$, and $\chi''(\mathbf{k}, \omega_{\mathbf{k}})$ is the imaginary part of the (semi-infinite) substrate density-density correlation function, as in electron energy loss [19]. Since $\mathbf{k} \cdot \mathbf{v}$ is a low frequency, a surge of friction near T_c is expected, in connection with the increased density of low frequency modes associated with softening of the displacive mode, and eventually with "central peak" diffusive excitations in the critical regime [9]. Without attempting to extract $\chi''(\mathbf{k}, \omega_{\mathbf{k}})$ from simulations, we note that since by Kramers-Kronig relations $\chi'(\mathbf{k} = 0, \omega = 0) = (2/\pi) \int_0^\infty \frac{\chi''(0,\omega)}{\omega} d\omega$, the T-dependent peak of χ' at T_c, while surely not identical to that of $\chi''(\mathbf{k}, \omega_{\mathbf{k}})$, should similarly accompany the peaking dissipation in this approximation. Results in Fig. 2 indeed qualitatively confirm a close similarity in the T dependence of simulated stick-slip friction with that independently obtained for the bulk susceptibility.

Further insight in the order-parameter valley dependence of friction can be obtained by inspecting the system's dynamics. The slider imparts mechanical kicks to nearby substrate atoms (details in supplemental material [13]) following which, energy is transmitted to the substrate and degraded as Joule heat (movies in supplemental material [13]). When T is low and the load is light the kicked substrate atoms vibrate moderately, harmonically, and mainly radially along the same potential valley; see diagram (i) of Fig. 2, resulting in very low friction. As the load increases, still at low temperatures, the sliding tip causes local order-parameter flips—jumps between valleys $\lambda \rightarrow \lambda'$—of near-tip atoms in the substrate. The work spent by the tip to actuate this local flip is never returned to the tip; thus an increased flip rate reflects in an increased friction coefficient which is seen well below T_c.

As temperature is raised, spontaneous thermal flips of order parameter proliferate in the substrate, eventually exploding critically near T_c. This is in correspondence with a surge of susceptibility, and to a drop of the free energy barrier for the tip to cause additional sliding-induced flips; so while their number also proliferates, see supplemental material [13], the friction rises to a critical maximum. (It should be noted, however, that some additional role in friction near T_c will be played by the muted propagation conditions of Joule phonons injected into the substrate, where propagation may be impeded by critical fluctuations.) Well above T_c finally all substrate atoms spontaneously and frequently jump over the six valleys [diagram (iii) in Fig. 2], offering a diminishing probability for the slider's kicks to do work, and friction gradually declines. The efficiency of stick slip in causing an order-parameter flip well below T_c is clearly not the same for different valleys λ. Figure 5 in the supplemental material [13] shows that flips between valleys are more abundant when the substrate is initially polarized in $\lambda = 2$ (or 1, 3, 4) than those with $\lambda = 6$ (or 5). The force exerted by the slider at slip is mostly downward oriented, thus valleys $\lambda = 2, 3$ can be kicked to $\lambda' = 1, 4$ (or even $\lambda' = 5, 6$); valleys $\lambda = 1, 4$ can be kicked to $\lambda' = 5, 6$; but valleys $\lambda = 5, 6$ cannot be kicked anywhere. The frictional differences between order-parameter directions become, we find, even larger when the load is raised as shown in Fig. 2, lower panel. All observations remain essentially the same for a lighter mass tip, see supplemental material [13]. Although schematic, the valley-specific efficiency

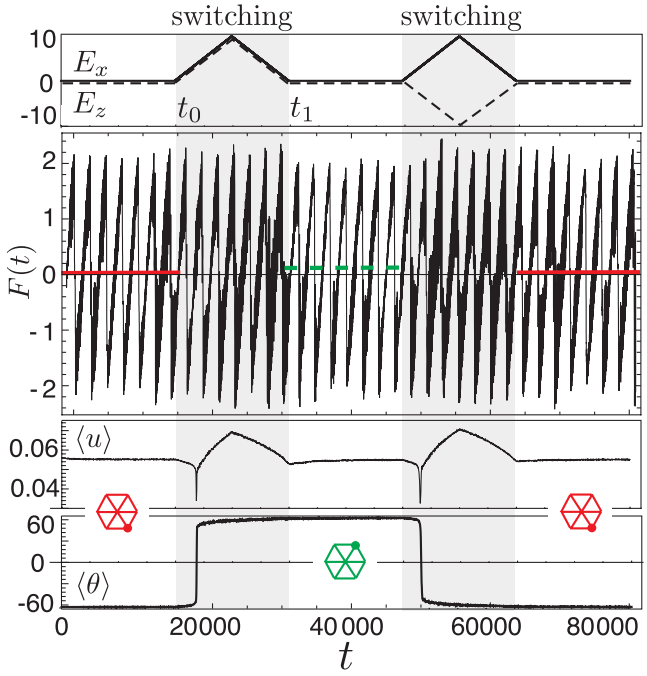

FIG. 3 (color online). Control of atomic stick slip upon application of an external field, switching the overall distortion direction from $\lambda = 6$ to $\lambda' = 2$. Upper panel, applied external field versus time; large panel, stick-slip friction force; continuous (red) and dashed (green) lines, average friction force. Note the "braking" effect. Lower panels, magnitude and orientation of the substrate order parameter. Simulations performed at $k_B T = 0.025U$ with $F_0 = 1.5$ and $v_0 = 5 \times 10^{-4}$.

difference in dissipation anticipates a general mechanism for the stick-slip friction dependence on the detailed domain orientation of the substrate order parameter, and a source of AFM frictional contrast between different domains.

This observation suggests a possible root to control friction, exemplified by the simulation of Fig. 3. Start out with the substrate polarized in valley $\lambda = 6$, where the low temperature stick-slip friction is small. At time $t = t_0$, an external field $\mathbf{E} = [E_x(t), E_z(t)]$, coupling to the order-parameter in the form $\mathbf{u} \cdot \mathbf{E}$, is turned on until $t = t_1$, when it is turned off. (For a ferroelectric substrate, $\mathbf{E}$ is an electric field; for ferrodistortive systems, it could be, e.g., a uniaxial deformation.) For sufficiently large field, the substrate overall distortion switches from valley $\lambda = 6$ to $\lambda' = 2$, and the friction correspondingly jumps upwards. Upon subsequent application of a restoring field $\mathbf{E} = [E_x(t), -E_z(t)]$, friction reverts back to low.

In summary, we have explored the behavior of the order-parameter-related friction qualitatively expected for stick-slip sliding over a structurally "live" substrate. While quantitatively model dependent, we obtained answers to our three basic questions (i)–(iii) which by all signs are of wider validity. The relative magnitude and detectability of the order-parameter-related frictional effects are by necessity system dependent and hard to predict. On the other hand the realm of solids exhibiting (nearly) continuous structural transitions is huge [10]. The domain contrast seen on ferroelectric $BaTiO_3$ [8] and on ferroelastics such as gadolinium molybdate (GMO) [20] and $RbAlF_4$ [21] could be pursued by temperature studies close to the ferro-para transitions. Antiferrodistorters like $SrTiO_3$ ($T_c \sim 105$ K) [22], and antiferroelectrics such as $KMnF_3$ ($T_c \sim 187$ K) [23] would also be of interest. The choice between these or other materials will largely be dictated by experimental considerations; and so will their potential use towards realistic control over dry friction.

This work is part of Eurocores FANAS/AFRI sponsored by the Italian Research Council (CNR). It is also sponsored by the Italian PRIN Contracts No. 20087NX9Y7 and No. 2008Y2P573. Discussions with H. Hug and D. Passerone are gratefully acknowledged.

[1] B. N. Persson, *Sliding Friction* (Springer-Verlag, Berlin, Germany, 1998).
[2] T. Ala-Nissila, W. K. Han, and S. C. Ying, Phys. Rev. Lett. **68**, 1866 (1992).
[3] T. Ala-Nissila, R. Ferrando, and S. C. Ying, Adv. Phys. **51**, 949 (2002).
[4] S. Prestipino, G. Santoro, and E. Tosatti, Phys. Rev. Lett. **75**, 4468 (1995).
[5] M. Kisiel *et al.*, Nature Mater. **10**, 119 (2011).
[6] A. Dayo, W. Alnasrallah, and J. Krim, Phys. Rev. Lett. **80**, 1690 (1998).
[7] A. Correia *et al.*, Appl. Phys. Lett. **68**, 2796 (1996).
[8] L. Eng *et al.*, J. Vac. Sci. Technol. B **14**, 1191 (1996).
[9] R. A. Cowley, Adv. Phys. **29**, 1 (1980).
[10] M. E. Lines and A. M. Glass, *Principles and Applications of Ferrolectrics and Related Materials* (Oxford University Press, Oxford, 1977).
[11] Fine details of the substrate critical behavior are purposely ignored here. We deliberately limit time and size in the simulation so as to avert the undesired Berezinskii-Kosterlitz-Thouless behavior [12].
[12] J. V. José *et al.*, Phys. Rev. B **16**, 1217 (1977).
[13] See supplemental material at http://link.aps.org/supplemental/10.1103/PhysRevLett.106.256102 for characterization of the displacive phase transition, of the kicking stick-slip dynamics with substrate energy flow, and for an analysis of the order-parameter flips.
[14] A. Benassi *et al.*, Phys. Rev. B **82**, 081401 (2010).
[15] E. Gnecco *et al.*, Phys. Rev. Lett. **84**, 1172 (2000).
[16] C. M. Mate *et al.*, Phys. Rev. Lett. **59**, 1942 (1987).
[17] Z. Tshiprut, S. Zelner, and M. Urbakh, Phys. Rev. Lett. **102**, 136102 (2009).
[18] I. Barel *et al.*, Phys. Rev. Lett. **104**, 066104 (2010).
[19] D. Pines, *Elementary Excitations in Solids* (Perseus Books, Reading, Massachusetts, 1999).
[20] R. Czajka *et al.*, Wear **238**, 34 (2000).
[21] A. Bulou and J. Nouet, J. Phys. C **15**, 183 (1982).
[22] K. A. Müller and W. Berlinger, Phys. Rev. Lett. **26**, 13 (1971).
[23] V. J. Minkiewi and G. Shirane, J. Phys. Soc. Jpn. **26**, 674 (1969).